Catalytic oxidation of polycyclic aromatic hydrocarbons (PAHs) over SBA-15 supported metal catalysts

Park, Joo-Il
Institute for Materials Chemistry and Engineering, Kyushu University

Lee, Jihn-Koo
PureSphere Co. Ltd., Korea Research Institute of Bioscience and Biotechnology

Miyawaki, Jin
Institute for Materials Chemistry and Engineering, Kyushu University

Yoon, Seong-Ho
Institute for Materials Chemistry and Engineering, Kyushu University

他

出版情報：Journal of Industrial and Engineering Chemistry. 17 (2), pp.271-276, 2011-03-25. Elsevier
バージョン：

Catalytic Oxidation of Polycyclic Aromatic Hydrocarbons (PAHs) over SBA-15 Supported Metal Catalysts

Joo-Il Park[a], Jihn-Koo Lee[b], Jin Miyawaki[a],
Seong-Ho Yoon[a]* and Isao Mochida[a]

[a]Institute for Materials Chemistry and Engineering, Kyushu University,
Fukuoka 816-8580, Japan
[b]PureSphere Co. Ltd.,121 Bio-venture Center, Korea Research Institute of Bioscience and Biotechnology, 52 Eoun-dong, Yuseong-gu, Daejeon 305-806, Republic of Korea

Tel.: +81-92-583-7959 , FAX .: +81-92-583-7897
e-mail : yoon@cm.kyushu-u.ac.jp

* : To whom correspondence should be addressed.

Abstract

Naphthalene was chosen as a model reactant of PAHs, and its catalytic destruction aimed to reduce the content of PAHs in diesel fuels was investigated over three different metal (Pt, Ru and Mo) catalysts supported on SBA-15 and γ-alumina. The catalysts were characterized by N_2-sorption isotherms, CO & NO chemisorptions, temperature programmed desorption of naphthalene & NH_3, and ^{27}Al MAS NMR. The SBA-15 supported metal catalysts showed a better activity at lower reaction temperature than the γ-alumina supported ones, most probably due to higher metal dispersion and enhanced meso-accessibility. Pt/SBA-15 catalyst exhibited the highest activity, corresponded to Ru or Mo/SBA-15 catalyst, as reasoned by the temperature programmed desorption of naphthalene. The improved catalytic performances and thermal stability of catalysts could be achieved by incorporation of Al species into SBA-15. The characteristics of Pt states and complex on the surface of acidic supports could lead to the enhanced catalytic activity of naphthalene oxidation, as well as the limited sintering of Pt particles at high temperature, giving rise to thermal stability of catalysts

Keywords: Polycyclic aromatic hydrocarbons(PAHs), Catalytic oxidation, SBA-15, Al-SBA-15

1. Introduction

Polycyclic aromatic hydrocarbons (PAHs) emitted from diesel engines are ubiquitous carcinogenic substances to which humans are exposed from the environment [1]. They are listed as carcinogenic and mutagenic priority pollutants, belonging to the environmental endocrine disrupters. Most PAHs stem from the atmospheric deposition and diesel emission. Consequently, the elimination of PAHs in the sources is one of the priority and emerging challenges. Among the PAHs, naphthalene is the most volatile member of this class of pollutants [2] and also a constituent of diesel and jet fuel [3-5]. Li et al. [4] and Siegl et al. [5] have pointed out that the PAHs in diesel emissions mainly consisted of two to five aromatic rings, especially, naphthalene, phenanthrene and pyrene. Most of the naphthlene is released into the atmosphere (90%), with a small portion into water (5%) and soil (3%) [3].

Common methods applicable for eliminating naphthalene from the waste stream include biodegradation [6], absorption [7], adsorption [8], ozonization [9,10] and catalytic oxidation[11,12]. Among them, the catalytic oxidation has been demonstrated as one of the cost effective and efficient technologies to destroy the troublesome VOCs. There are very few reports on the catalytic oxidation of naphthalene, mostly on the γ-alumina supported metal catalysts [11,12].

Zhang et al. [11] have investigated the activities of precious metal and transition metal in decomposing naphthalene and discussed the reaction kinetics on Pt supported γ-alumina catalyst. For the catalytic oxidation of naphthalene using Pt supported γ-alumina catalysts, Shie et al. [12] have studied the relationships between conversion, operating parameters and relevant factors such as treatment temperatures, catalyst size and space velocities. Since the catalytic activities for naphthalene oxidation has been reported to be very effective only at high temperature over 300^{o}C, it is desirable to develop good catalyst functioning at lower temperature.

Supported Ru catalysts have been received much attention over the past years, because of their high activity in oxidation as well as reduction reactions. Actually, they have been proved to be among the best catalytic systems for oxidation of various substrates such as methane [13, 14],carbon monoxide [15-17], ammonia [18], hydrogen [19], alcohols [20], diesel soot [21], and even HCl in low temperature oxidation [22].

In addition, for the clear comparison of differences of catalytic oxidation, corresponded to Ru catalysts, we have considered the Mo active metal, which has been known as the partial oxidation of naphthalene to quinines and dicarboxylic anhydrides.

In this work, metal (Pt, Ru, Mo) containing catalysts were prepared using the mesoporous silica SBA-15 as a support material due to its good thermal and

hydrothermal stability, high surface area, and narrow pore size distribution, and their catalytic activities for naphthalene oxidation were investigated, comparing to the conventional γ-alumina supported metal catalysts. Furthermore, the enhanced catalytic activity as well as the thermal stability has been surveyed by the incorporation of Al species into SBA-15.

2. Experimental

2.1. Preparation of catalysts

The SBA-15 support was prepared according to a procedure described in literature by Stucky et al. [23]. Pluronic 123 ($EO_{20}PO_{70}EO_{20}$) was dissolved in 1.6 M HCl solution with stirring. After 1 h, the silica source, tetraethylorthosilicate (TEOS), was added in the tri-block copolymer solution and stirred for 1 h at 35^{o}C. The mixture was reacted at 35^{o}C for 24 h and subsequently at 100^{o}C for 12 h. The precipitates were filtered, washed with distilled water, dried in an oven at 100^{o}C, and then calcined in air at 550^{o}C for 5 h.

Al-SBA-15 was prepared by incorporating aluminum to siliceous SBA-15 by the post synthetic metal implantation method. Siliceous SBA-15 was heated to remove water in a vacuum oven at 100^{o}C for 10 h. $AlCl_3$ anhydrate (Junsei, reagent grade) in absolute ethanol (99.8 wt %, Merck) was added to siliceous SBA-15 in polypropylene bottle and the mixture was stirred vigorously for 30 min. The mixture was filtered, washed with absolute ethanol and dried at 110^{o}C in air. Calcination was done in a muffle type furnace and the temperature was increased to 550^{o}C over 10 h and hold at 550^{o}C for 5 h. The Si/Al ratios of Al-SBA-15 were chosen to be 10, 15, and 90.

Supported metal catalysts were prepared by incipient wetness impregnation method. $Pt(NH_3)_4Cl_2 \cdot H_2O$ (98%, Aldrich), $RuCl_3 \cdot H_2O$ and $(NH_4)_6Mo_7O_{24} \cdot 4H_2O$ were used as metal precursors, respectively, and 1 wt% of Pt, 1 wt% of Ru and 5 wt% of Mo were loaded on the silica or γ-alumina supports by incipient wetness method, and they were dried at 100°C and calcined at 550°C for 5 h.

2.2. Characterization

The physical properties of the calcined catalysts including BET specific surface area, pore volume and pore size distribution were determined using an ASAP 2010 volumetric sorption analyzer (Micomeritics Inc., USA). The samples were degassed at 200°C, and the nitrogen adsorption/desorption isotherm measurements were carried out at 77 K. Surface areas were measured by the linear region of the Brunauer-Emmett-Teller (BET) plots and the pore size distribution was analyzed by the Barrett-Joyner-Halenda (BJH) method using a desorption branch of the isotherm.

The acidity of Al-SBA-15 was analyzed by temperature programmed desorption (TPD) of NH_3 with Pulse Chemisorb 2705 (Micomeritics Inc., USA). Before the adsorption of NH_3, the samples of 5 mg loaded in the U-type quartz tube were pretreated at 500°C with He flow of 20 ml/min for 2 h, and cooled down to 100°C.

After the saturation, the samples were heated at a rate of 5^{o}C/min from 100^{o}C to 600^{o}C, and the TCD signal from desorbed NH_3 was recorded.

The ^{27}Al NMR spectra of synthesized mesoporous molecular sieves were obtained with 400 MHz solid state FT-NMR spectrometer (DSX 400MHz Bruker Analytische GmbH). The spectra were measured at 79.5 MHz. The chemical shifts were referenced to $[Al(H_2O)_6]_3$ for ^{27}Al.

Pt and Ru dispersions were determined by CO chemisorption with ASAP 2010C (Micromeritcis) and Mo dispersion by NO chemisorptions [24-28] with Pulse Chemisorb 2705 (Micomeritics Inc., USA).

Temperature programmed desorption of naphthalene was conducted by monitoring the naphthalene concentration at the outlet of reactor via an on-line GC-MS (5971, Hewlett-Packard, USA). After purging with He (50ml/min) at 500^{o}C for 3 h, the reactor was cooled down to 100^{o}C. Naphthalene was then introduced into the reactor. When the catalysts were saturated with naphthalene, He (30ml/min) was flown to eliminate the physically adsorbed naphthalene from the catalysts. Then the TPD spectra of chemisorbed naphthalene on the catalysts were obtained as a function of temperature.

2.3. Catalytic activities

The catalytic activity for the oxidation of naphthalene was measured using a fixed bed apparatus at a temperature range of 150^{o}C to 500^{o}C and at a time-on-stream of 2 h. The reaction stream (400 ppmv naphthalene with balance air) was introduced through the evaporator at 100^{o}C. The schematic of reaction apparatus is shown in Figure 1. The space time (W/F) was 0.016 g-cat·h/L. The effluent gases were analysed by a on-line GC (6890, Hewlett-Packard, USA) through HP-5 column with FID for naphthalene and other hydrocarbons, and Carboxene 1006 column for CO and CO_2 with methanizer. The conversion of naphthalene and CO_2 yield [$(CO_2)_e/(CO_2)_t \times 100$, %] were measured as a function of temperature. Here, $(CO_2)_e$ denotes the CO_2 concentration which was measured experimentally and $(CO_2)_t$ the one stoichiometrically predicted for complete oxidation of naphthalene ($C_{10}H_8 + 12O_2 \rightarrow 10CO_2 + 4H_2O$). The activity data were obtained after 2 h stabilization at a given temperature.

3. Results and discussion

3.1. Catalytic decomposition of naphthalene

The BET surface area, pore volume and pore size distribution determined by nitrogen physisorption of the prepared catalysts summarized in Table 1. The SBA-15 supported metal catalysts were found to have narrower pore size distribution, higher BET surface areas, as well as larger pore volume than those of the γ-alumina supported metal catalysts.

In Figure 2, the temperatures of 95% conversion of naphthalene and CO_2 yield over Pt/SBA-15 were 190^{o}C and 290^{o}C, respectively, while those of Pt/γ-alumina were 290^{o}C and 400^{o}C. In the case of Ru and Mo catalysts, temperatures indicating 95% conversion of naphthalene and CO_2 yield were much higher. Hence, Pt/SBA-15 or γ-alumina were obviously more favorable than Ru and Mo catalysts for naphthalene complete oxidation. Considering to supports, the SBA-15 supported metal catalysts showed better activity for oxidation of naphthalene at lower temperature than γ-alumina supported metal catalysts. The enhanced oxidation activity of the SBA-15 supported metal catalysts could be related to better metal dispersion resulted from mesopore character as shown in Table 1. Generally, ordered mesoporous silica has been widely studied as supports for catalysts [29, 30] or as a matrix for the preparation of nanosized,

high surface area materials [31-34]. These materials have not only a high surface area (up to 1000 m^2/g), but also a narrow pore size distribution. The advantage of metal particles confined inside the supports lies in the high dispersion of the metal itself, an increased resistance sintering [35-38]. Therefore, the well dispersion of the active metals in SBA-15 could be considered to be due to the mesopore characteristics of the supports, giving rise to better catalytic performances.

Although metal catalysts supported on SBA-15 showed better activity at lower temperature than γ-alumina supported metal catalysts, both catalysts represented the deficit in the carbon balance at each temperature. It implies the incomplete oxidation to CO_2 which can be led to the generation of secondary pollutants as a by-product. This deficit of carbon balance is dependent on the reaction temperature and on the catalysts used. In consequence, good catalysts lowering the temperature for completely converting into CO_2 would be demanded. Weber et al. [39] have reported that V_2O_5-WO_3/TiO_2 catalysts were active in decomposing polychlorinated dibenzo-p-dioxins (PCDDS), polychlorinated dibnenzofurans (PCBZs), and PAHs (such as biphenyl and pyrene). They showed that the converted reactants may generate by-products as secondary pollutants, indicating the partial conversion to CO_2. It has also been observed by Zhang et al [11]. These authors showed that during naphthalene decomposition over

Pt catalysts, little carbon dioxide was produced at 200^{o}C, while more than 50% of the naphthalene was consumed, suggesting that naphthalene was partially converted to other by-products. Since the destruction of reactants may generate byproducts as secondary pollutants, the disappearance of reactants does not always represent the extent of complete oxidation. In fact, our GC-MS analyses confirmed that a larger amount of intermediate hydrocarbons was yielded at 200^{o}C, but the complicated compositions of byproducts made quantitative analyses difficult. Therefore, the catalyst activity based on final products such as CO_2 was adopted as an index to estimate the catalytic activity in this study.

The catalytic activity for naphthalene complete oxidation followed the sequence of Pt(1)/SBA-15 > Ru(1)/SBA-15 > Mo(5)/SBA-15 among the metal/SBA-15 catalysts. The reactivity of different metals have been reasoned with the TPD spectra of naphthalene as shown in Figure 3. No desorption of chemisorbed naphthalene was observed for pure SBA-15 support, indicating the physically adsorbed naphthalene over SBA-15 support, thereby removing below 150^{o}C. The desorption peak of naphthalene with Pt catalyst was at around 200^{o}C. For Ru catalyst, the naphthalene desorption peaked at around 230^{o}C with a tail up to about 470^{o}C. The Mo catalyst, however, showed a broad desorption pattern ranged from 130^{o}C to 470^{o}C, suggesting that

naphthalene chemisorbed more strongly on the Mo/SBA-15. To summarize, naphthalene was completely desorbed from the Pt/SBA-15 catalyst at much lower temperature, indicating a weak chemisorption, which could be led to the higher activity than Ru or Mo/SBA-15.

3.2. Al incorporation and thermal stability

Al-SBA-15 was prepared by incorporating aluminum to siliceous SBA-15 supports by the post synthetic metal implantation method. Physical properties of prepared Pt/Al-SBA-15 catalysts were listed in Table 2, in which surface area and pore volume were decreased with increasing amount of Al.

The ^{27}Al MAS NMR spectra of Al/SBA-15 were shown in Figure 4. The peak fitting results of NMR spectra are summarized in Table 3. The peaks were assumed by the form of Gaussian distribution. The ^{27}Al MAS NMR spectra of the supports showed peaks at 50 ppm (tetrahedrally coordinated Al, Al(IV) in the framework) and 0 ppm (octahedrally coordinated Al, Al(VI) at extra-framework) of chemical shift, respectively [40, 41]. The chemical shift (30 ppm) related to the deformation of some Al(IV) sites did not appeared. The percentage of the octahedral Al sites became significant with lower Si/Al molar ratio. NMR results indicate that considerable amounts of aluminum

were successfully incorporated into the framework of SBA-15, and also the octahedral Al species on the surface of SBA-15, which were located at accessible outer sites, significantly increased with Al content.

Figure 5 shows that the catalytic activity for naphthalene oxidation over Pt/SBA-15 was improved by the Al incorporation. Comparing to the conversion of naphthalene over Pt/Al-SBA-15 did not increase remarkably, CO_2 yield was shifted significantly to lower temperature, indicating higher activity on oxidation of naphthalene with less by-product formation than Pt/SBA-15. Improvement of the activity could be reasoned by the enhancement of surface acidity which was evidenced by NH_3-TPD, as shown in Figure 6; amount of acid sites of Al-SBA-15 increased with decreasing Si/Al ratios as expected. Y. Yazawa et al. [42] suggested that acid sites of the support materials largely affects on the catalytic activity than the degree of Pt dispersion during the propane combustion, thereby being improved the catalytic activity by more acidic support materials. The higher activity may come from the differences in the oxidation state of the Pt catalyst by the support materials; Pt on the acidic supports is less oxidized than that on the basic ones, suggesting the higher oxidation-resistance. In this sense, the higher oxidation activity of Pt/Al-SBA-15 could be explained as the higher oxidation-resistance of Pt over acidic support.

Even if high catalytic activity of Pt-based catalysts has been confirmed, the investigation of the thermal stability of Pt/SBA-15 catalyst is also of importance for needs to be applied under real operation condition and temperature in the catalyst bed, which can rise to over 800^{o}C during a normal operation of an engine. For the consideration of thermal stability, the catalytic activity over Pt/SBA-15 and Pt/Al-SBA-15 catalysts calcined at different temperature were investigated. After being aged in air at 800^{o}C for 5h, catalytic activities of Pt/SBA-15 and Pt/Al-SBA-15 were found to decrease, as shown in Figure 7. All catalysts calcined at 550^{o}C were kept over 95% CO_2 yield at 290^{o}C. Even if CO_2 yield over Pt/SBA-15 decreased from 97.0% to 72.5%, the reduction of CO_2 yield over Pt/Al-SBA-15 catalysts after aging 800^{o}C was only less than 10%, which was much smaller than that of Pt/SBA-15. This thermal stability of Pt/Al-SBA-15 catalyst could be provided since the surface Al species prevented the active Pt species from sintering at higher temperature. The CO chemisorption results showed that the change of metal dispersion due to calcination at 800^{o}C was significantly inhibited in the Pt/Al(90, 15, 10)-SBA-15 catalyst (i.e., 31 %→ 26 %, 25 % → 22 %, and 23 %→20 %, respectively), while the Pt/SBA-15 showed the considerable decrease in the dispersion (i.e., 35% → 19%). It has been reported that Cl^- ligands in Pt complex such as $[PtCl_6]^{2-}$ and $[PtCl_5(OH)]^{2-}$ exchanged with the hydroxyl groups on the alumina

surface [43, 44]. Furthermore, This Pt complex is adsorbed irreversibly on the alumina surface by drying at 90^{o}C [44]. In contrast, the hydroxyl group on the silica surface (Si-OH) also act as a ligand of Pt complex, but Si-OH ligand in Pt complex exchanged reversibly with H_2O even after drying at 90^{o}C [45]. These results indicate that the interaction between Pt particles and Al-modified silica surface is stronger than that of the silica surface. Therefore, inhibition of Pt sintering could be significantly enhanced by Al modified SBA-15.

4. Conclusion

The well dispersion of the active metals over mesoporous support (SBA-15) led to higher catalytic activity of naphthalene complete oxidation at lower temperature, comparing to the conventional γ-alumina supported ones. Among the SBA-15 supported metal catalysts, Pt was more active than Ru or Mo, due to weak chemisorption of naphthalene. The presence Al species either in the framework or on the surface of SBA-15 support was found to improve the activity of Pt/SBA-15, which could be attributed to the less oxidized Pt species on the acidic supports of Al-SBA-15. The incorporated Al species could be also considered to work as a structural promoter for limiting the sintering of Pt metals at high temperature, being explained by the Pt complex adsorbed irreversibly on the alumina, as well as its strong interaction between Pt and Al-modified silica surface.

5. References

[1] Inernational Program on Chemical Safty(IPCS), Environmental Health Criteria 2002, Selected Non-heterocyclic Polycyclic Aromatic Hydrocarbons, WHO, Geneva (1998)

[2] R. Preuss, J. Angerer, and H. Drexler, Int. Arch. Occup. Environ. Health 76 (2003) 556

[3] S. Coons, M. Byrne, and M. Goyer, An Exposure and Risk Assessment for Benzo(a)pyrene and Other Polycyclic Aromatic Hydrocarbons: vol. II. Naphthalene, Final Draft Report, USEPA, Office of Water Regulations and Standards, Washington, DC, (1982)

[4] H. Li, C.D. Banner, G.G. Mason, R.N. Westerholm, and J.J. Rafter, Atmos. Environ. 30 (1996) 3537

[5] W.O. Seigl, R.H. Hammerle, H.M. Herrmann, B.W. Wenclawiak, and B. Luers-Jongen, Atmos. Environ. 33 (1999) 797

[6] G. Chen, K.A. Strevett, and B.A. Vanegas, Biodegradation 12 (2001) 433

[7] H. Lhuang, and W.M. Lee, J. Environ. Eng. ASCE 128 (2002) 60

[8] S.Y. Lee, and S.J. Kim, Appl. Clay Sci. 22 (2002) 55

[9] B. Legube, S. Guyon, H. Sugimitsu, and M. Dore, Water Res. 20 (1986) 197

[10] Y. Hchen, C.Y. Chang, S.F. Huang, C.Y. Chiu, D. Ji, N.C. Shang, Y.H. Yu, P.C. Chiang, Y. Ku, and J.N. Chen, Water Res. 36 (2002) 4144

[11] X.W. Zhang, S.C. Shen, L.E. Yu, S. Kawi, K. Hidajat, and K.Y.S. Ng, Appl. Catal. A: Gen. 250 (2003) 341

[12] J.L. Shie, C.Y. Chang, and J.H. Chen, Appl. Catal. B: Environ. 58 (2005) 289

[13] I. Balint, A. Miyazaki, K. Aika, J. Catal. 220 (2003) 74

[14] Y. Liu, F.-Y. Huang, J.-M. Li, W.-Z. Weng, Ch.-R. Luo, M.-L. Wang, W.-S. Xia, Ch.-J. Huang, H.-L. Wan, J. Catal. 256 (2008) 192

[15] H. Over, Y.D. Kim, A.P. Seitsonen, S. Wendt, E. Lundgren, M. Schmid, P. Varga, A. Morgante, G. Ertl, Science 287 (2000) 1474.

[16] J. Assmann, V. Narkhede, N.A. Breuer, M. Muhler, A.P. Seitsonen, M. Knapp, D. Crihan, A. Farkas, G. Mellau, H. Over, J. Phys.: Condens. Matter 20 (2008) 184017

[17] K. Reuter, M. Scheffler, Phys. Rev. B 73 (2006) 045433

[18] Y. Wang, K. Jacobi, W.-D. Schoene, G. Ertl, J. Phys. Chem. B 109 (2005) 7883

[19] M. Knapp, D. Crihan, A.P. Seitsonen, E. Lundgren, A. Resta, J.N. Andersen, H. Over, J. Phys. Chem. C 111 (2007) 5363

[20] H. Liu, E. Iglesia, J. Phys. Chem. B 109 (2005) 2155

[21] M. Dhakad, S. Rayalu, J. Subrt, S. Bakardjieva, T. Mitsuhashi, N. Labhsetwar, Curr. Sci. 92 (2007) 1125

[22] N. López, J. Gómez-Segura, R.P. Marín, J. Pérez-Ramírez, J. Catal. 255 (2008) 29

[23] Y.J. Han, J.M. Kim, and G.D. Stucky, Chem. Mater. 12 (2000) 2068

[24] Wendy A. Brown and David A. King, J. Phys. Chem. B 104 (2000) 2578

[25] C.M. Friend and K.T. Queeney, ChemPhysChem 1 (2000) 116

[26] K.T. Oueeney, S. Pang, and C.M. Friend, J. Chem. Phys. 109 (1998) 8058

[27] K.T. Queeney and C.M. Friend, J. Phys. Chem. B 102 (1998) 9251

[28] K.T. Queeney and C.M. Friend, Surf. Sci. 414 (1998) L957

[29] A. Taguchi, F. Schuth, Micropor. Mesopor. Mater. 77 (2005) 1.

[30] J. Sauer, S. Kaskel, M. Janicke, F. Schuth, Stud. Surf. Sci. Catal. 135 (2001) 315.

[31] F. Schuth, Chem. Mater. 13 (2001) 3184.

[32] P. Krawiec, C. Weidenthaler, S. Kaskel, Chem. Mater. 16 (2004) 2869.

[33] R.S. Ryoo, H. Joo, M. Kruk, M. Jaroniec, Adv. Mater. 13 (2001) 677.

[34] P. Dibandjo, L. Bois, F. Chassagneux, D. Cornu, J.M. Letoffe, B. Toury, F.Babonneau, P. Miele, Adv. Mater. 17 (2005) 571.

[35] L. Zhang, G.C. Papaefthymiou, J.Y. Ying, J. Phys. Chem. B 105 (2001) 7414.

[36] E. Molnar, Z. Konya, I. Kiricsi, J. Therm. Anal. Calorim. 79 (2005) 573.

[37] F.W. Yan, S.F. Zhang, C.Y. Guo, F.B. Li, F. Yan, G.Q. Yuan, Catal. Comm. 10 (2009) 1689

[38] P. Papaefthimiou, T. Ioannides, and X.E. Verykios, Appl. Catal. B: Environ. 13 (1999) 175

[39] R. Weber, T. Sadurai, H. Hagemaier, Appl. Catal. B: Environ. 20 (1999) 249

[40] L.L.L. Prado, P.A.P. Nascente, S.C. De Castro, and Y. Gushikem, J. Mater. Sci. 35 (2000) 449

[41] L.Y. Chen, Z. Ping, G..K. Chuah, S. Jaenicke, and G. Simon, Micropor. Mesopor. Mater. 27 (1999) 231

[42] Y. Yazawa, N. Takagi, H. Yoshida, S. Komai, A. Satsuma, T. Tanaka, S. Yoshida, T. Hattori, Appl. Catal. A: Gen. 233 (2002) 103

[43] J.H.A. Maetens, R. Prins, Appl. Catal. 46 (1989) 31

[44] B. Shelimov, J.F. Lambert, M. Che, B. Didillon, J. Catal. 185 (1999) 462

[45] J.M. Fraile, J.I. Garcia, J.A. Mayoral, Catal. Lett. 88 (2003) 23

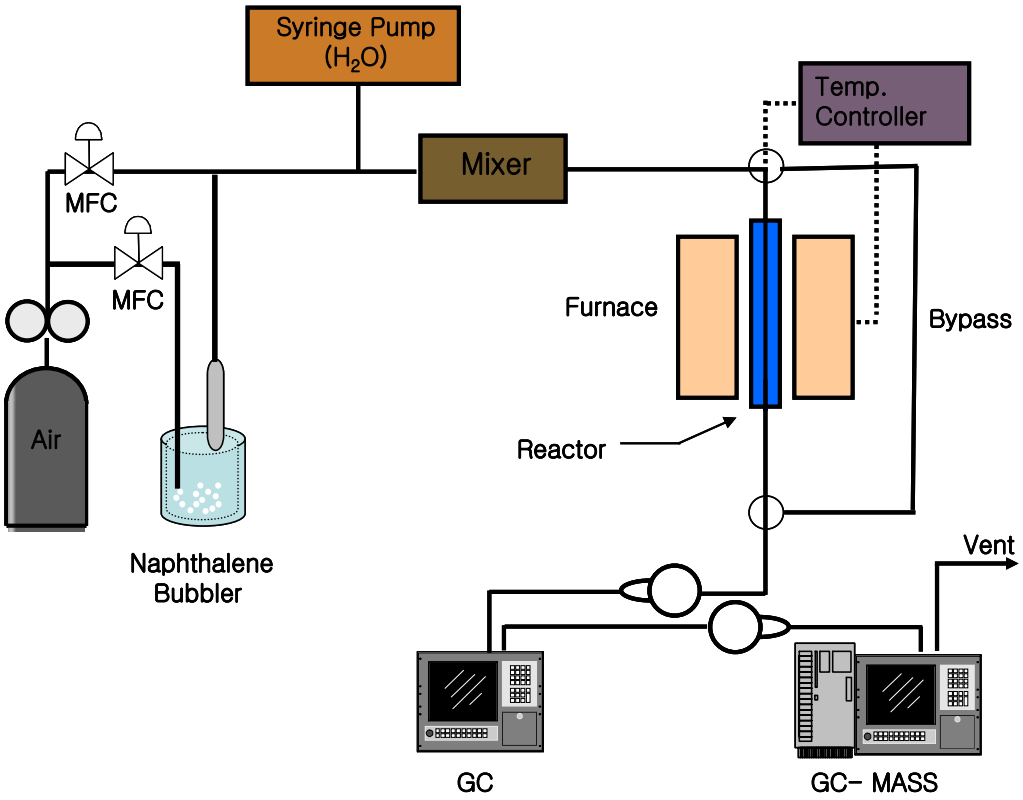

Figure 1. Reaction apparatus for catalytic decomposition of naphthalene

Table 1. The physical properties of SBA-15 and γ-Al_2O_3 supported metal catalysts.

Catalysts	Surface area (m^2/g)	Pore volume (cm^3/g)	Avg. Pore diameter (Å)	Metal dispersion [CO or (NO) chemisorption, %]
SBA-15	956	0.98	53.2	-
γ-Al_2O_3	184	0.27	50.5	-
Pt(1)*/SBA-15	920	0.95	52.3	35
Pt(1)/γ-Al_2O_3	169	0.25	49.9	18
Ru(1)/SBA-15	927	0.94	52.1	28
Ru(1)/γ-Al_2O_3	168	0.25	50.1	16
Mo(5)/SBA-15	657	0.84	48.8	(14)
Mo(5)/γ-Al_2O_3	137	0.19	47.9	(6)

*: metal loading(wt%)

Table 2. The physical properties of Pt/SBA-15 and Pt/Al-SBA-15 calcined at different temperature.

Catalysts	Surface area (m^2/g)	Pore volume (cm^3/g)	Avg. Pore diameter (Å)	Pt dispersion (CO chemisorption, %)
Pt/SBA-15(A)	920	0.95	52.3	35
Pt/SBA-15(B)	649	0.80	49.2	19
Pt/Al(90*)-SBA-15(A)	891	0.91	52.1	31
Pt/Al(90)-SBA-15(B)	877	0.90	51.7	26
Pt/Al(15)-SBA-15(A)	752	0.83	49.9	25
Pt/Al(15)-SBA-15(B)	731	0.79	50.1	22
Pt/Al(10)-SBA-15(A)	643	0.75	48.6	23
Pt/Al(10)-SBA-15(B)	598	0.72	48.3	20

*: Si/Al mole ratio, A: calcined at 550°C, B: calcined at 800°C

Table 3. The peak area percent of tetrahedral Al sites and octahedral Al sites for Al-SBA-15 from solid ^{27}Al MAS NMR

Si/Al molar ratio	Tetralhedral Al (%)	Octahedral Al (%)
90	65.5	34.5
10	58.8	41.2

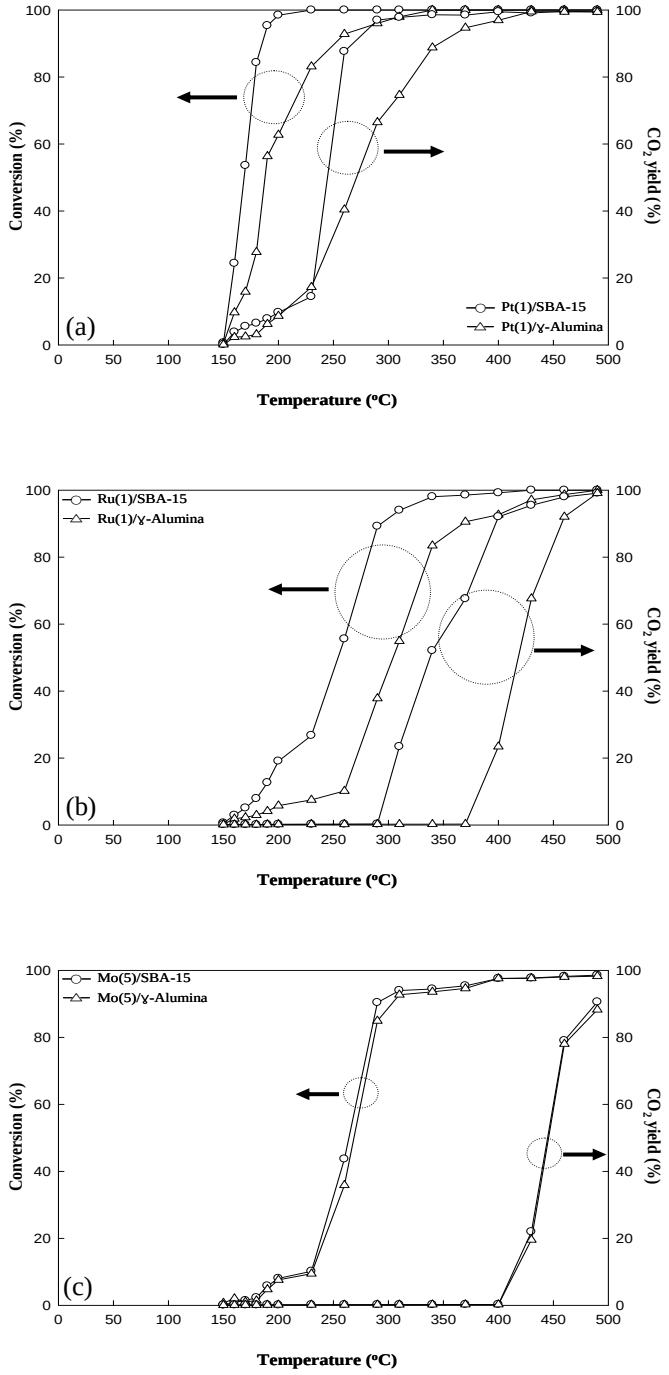

Figure 2. Conversion of naphthalene and CO_2 yield over (a) Pt(1)/SBA-15 and Pt(1)/ γ-alumina, (b) Ru(1)/SBA-15 and Ru(1)/ γ-alumina and (c) Mo(5)/SBA-15 and Mo(5)/ γ-alumina for catalytic oxidation of naphthalene

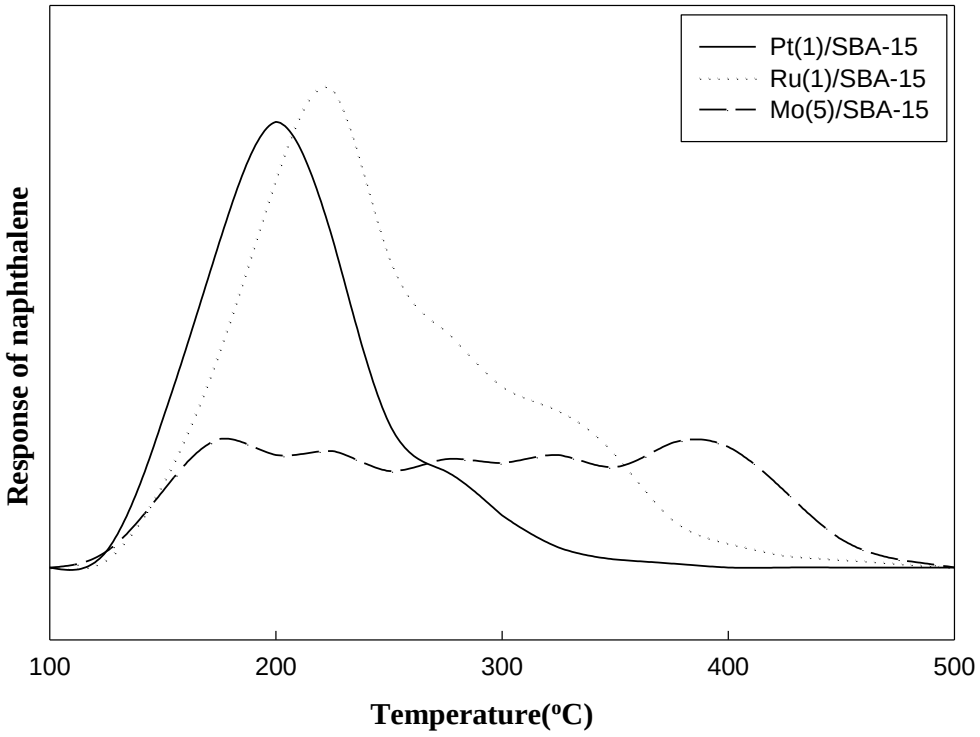

Figure 3. The temperature programmed desorption (TPD) of naphthalene from metal/SBA-15

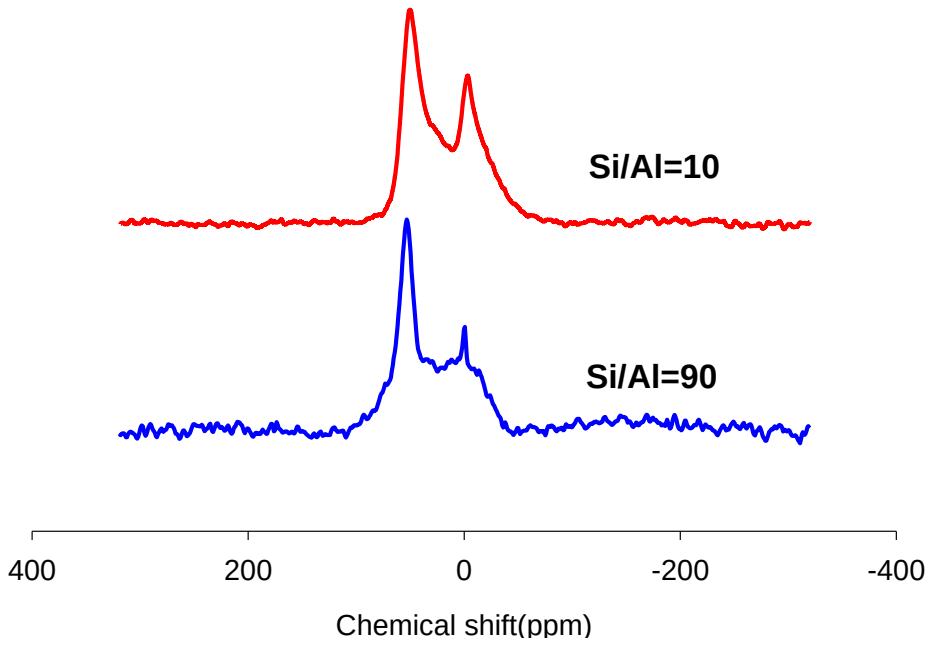

Figure 4. ^{27}Al MAS NMR spectra of Al-SBA-15 of different Si/Al ratio

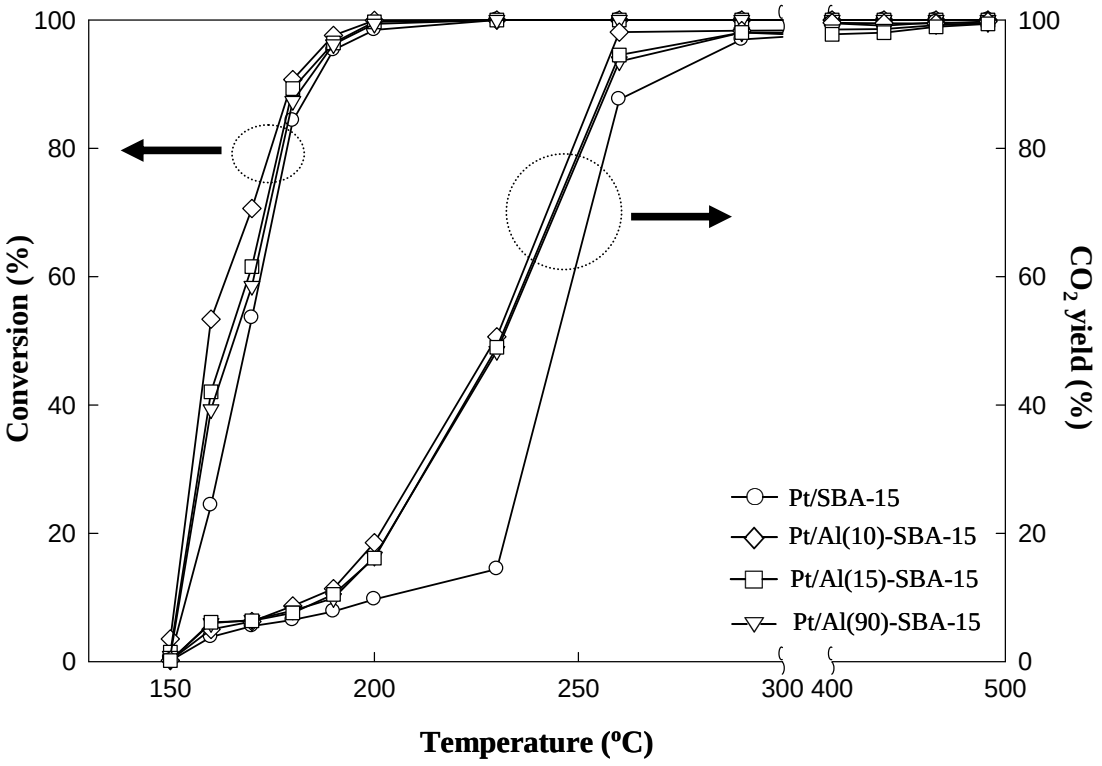

Figure 5. Conversion of naphthalene and CO_2 yield over Pt/SBA-15 and Pt/Al-SBA-15 catalysts for catalytic oxidation of naphthalene

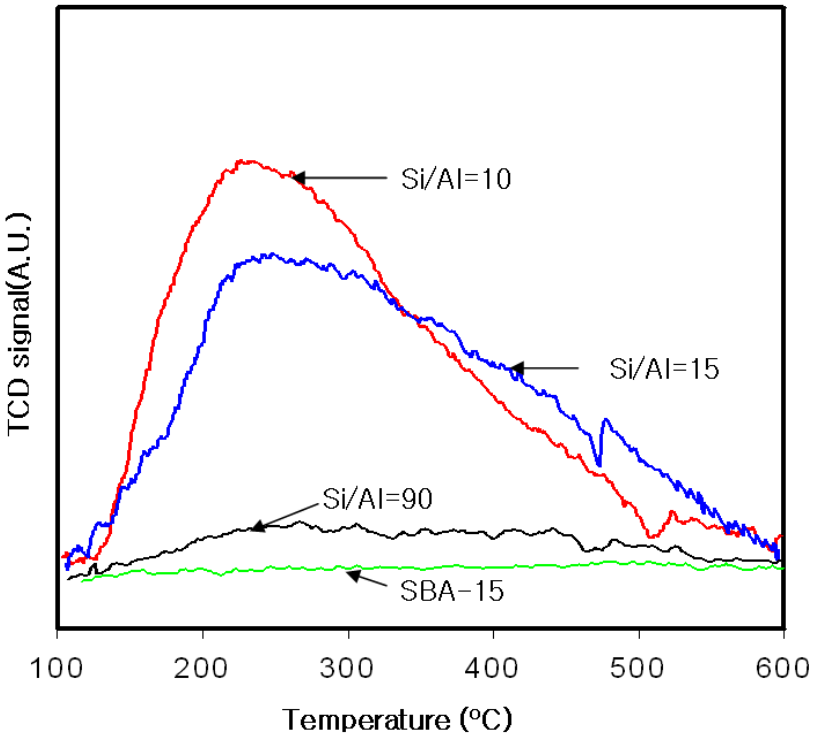

Figure 6. NH_3-TPD spectra of SBA-15 and Al-SBA-15

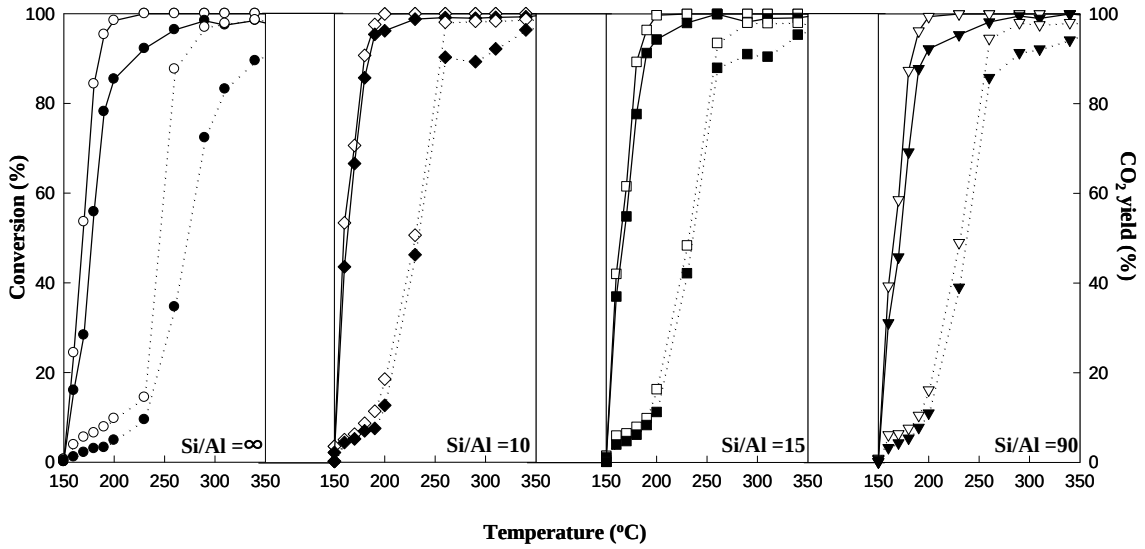

Figure 7. Conversion of naphthalene (solid line) and CO_2 yield (dotted line) over Pt/SBA-15 and Pt/Al-SBA-15 calcined at different temperatures; (Open symbols) 550^{o}C; (Closed symbols) 800^{o}C